ChemComm

Cite this: *Chem. Commun.*, 2012, **48**, 8904–8906

www.rsc.org/chemcomm

COMMUNICATION

Ultrafine nanofibers fabricated from an arylene–ethynylene macrocyclic molecule using surface assisted self-assembly†

Aniket Datar,[a] Dustin E. Gross,[b] Kaushik Balakrishnan,[ac] Xiaomei Yang,[d] Jeffrey S. Moore*[b] and Ling Zang*[ad]

Received 8th June 2012, Accepted 12th July 2012
DOI: 10.1039/c2cc34127a

Large area uniform nanofibers have been fabricated from a hexameric arylene–ethynylene macrocycle (1) through *in situ* self-assembly on a glass substrate during solvent evaporation. The fibril morphology is controlled by the solvophilic core of 1, in conjunction with the interfacial interactions between the side chains of 1 and the substrate.

Arylene–ethynylene macrocycles (AEMs) represent a unique class of building-block molecules due to their large π-surface, shape persistent, non-collapsible backbone, and an interior space which can range from less than ten up to *ca.* 100 angstroms.[1] Recently, we have demonstrated the utilization of AEMs as building blocks for functional optical and electronic sensory materials.[2,3] The shape persistent π-surface of AEMs favourably participates in intermolecular π-stacking interactions as observed in nanoporous crystals,[4–6] liquid crystals,[7–9] monolayers[10] and single crystals.[11] In spite of an apparent propensity to adopt long-range order, the occurrence of well-defined, one-dimensional (1D) self-assembly (*e.g.* nanofibers) from this class of macrocycles had rarely been reported until the first such nanostructures were fabricated from carbazole-based tetracyclic AEMs.[12,13] One major challenge for the 1D self-assembly is the steric hindrance of the bulky side chains attached to the aromatic core, which is appended to impart solubility. To overcome steric repulsion and maximize the π-stacking interactions, our group previously reported a novel self-assembly method based on temperature controlled gelation in a solvent of modest solubility.[12,13] However, the same gelation or solution processing may not be applicable to macrocycles that exhibit high solubility in a wide range of organic solvents. Additionally, the geometry of the macrocycle is expected to play a major role in the solution processability and propensity of nanofiber formation.[14]

Herein, we report on a novel approach based on surface assisted self-assembly to fabricate well-defined nanofibril structures from a *m*-phenylene ethynylene macrocycle appended with six oligoethylene glycol side chains (molecule **1** shown in Scheme 1). The amphiphilic property of **1** makes it soluble in most organic solvents, hindering the 1D self-assembly in solution phase, wherein a poor solvent is normally required to enable the aggregation. As shown in Scheme 1, surface assisted assembly, *via* solution casting followed by solvent evaporation, incorporates the interfacial interaction between the hydrophilic side chains and the glass surface, which enforces the vertical orientation of the macrocycle plane with respect to the substrate as previously evidenced,[10] thus facilitating the intermolecular π-stacking arrangement parallel to the substrate. The interfacial interaction also reduces the surface molecular mobility (random walking), resulting in enhancement of molecular assembly. Furthermore, the carbonyl linkage enforces a planar geometry between the linear side chains and the central macromolecular skeleton conducive to the cofacial π-stacking.[15]

As a preliminary investigation, 0.3 mM solutions of molecule **1** dissolved in four different solvents (chloroform, methanol, *p*-xylene and toluene) were *drop*-cast on glass slides, followed by evaporation at room temperature. The film thus formed was imaged with taping-mode AFM to reveal the nanoscale morphology (see Fig. S1, ESI†). Of these solvents only the toluene solution of **1** formed elongated nanostructures with a clear 1D morphology, *i.e.*, needle-like nanocrystals. We attribute this observation to the

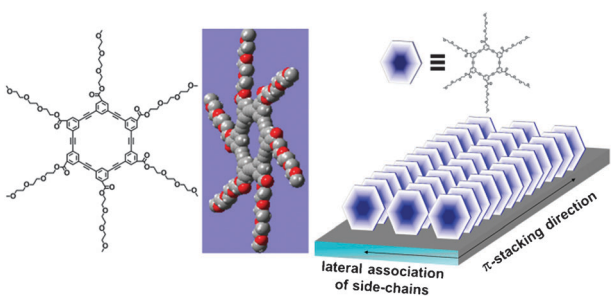

Scheme 1 Molecular structure of **1** and highly planar geometry revealed by *ab initio* calculations; schematic diagram on right shows 1D self-assembly induced by π–π stacking.

[a] *Department of Chemistry and Biochemistry, Southern Illinois University, Carbondale, IL 62901, USA*
[b] *Department of Chemistry, University of Illinois at Urbana–Champaign, Urbana, IL 61801, USA. E-mail: jsmoore@illinois.edu*
[c] *College of Optical Sciences, University of Arizona, Tucson, AZ 85721, USA*
[d] *Department of Materials Science and Engineering, University of Utah, Salt Lake City, UT 84108, USA. E-mail: lzang@eng.utah.edu; Fax: +1 801-585-0625; Tel: +1 801-587-1551*

† Electronic supplementary information (ESI) available: Large area AFM images of nanofibers, AFM investigation of drop-cast films from different solvents, cross-polarized optical images, XRD data. See DOI: 10.1039/c2cc34127a

effective wetting of toluene on the glass surface, as well as to the strong solvophilic interaction between **1** and toluene that provides the molecules with sufficient diffusivity to allow for self-assembly during the solvent evaporation process. The formation of similar 1D ordered nanostructures has been previously reported for alkyl chain substituted polycyclic discotic molecules such as triphenylenes, hexabenzocoronenes,[16] porphyrin trimers[17] and π-conjugated polymers,[16,18,19] through solvent evaporation on planar substrates. Solvent evaporation on desired substrates represents a simple and practical approach towards fabrication of large area ordered 1D nanostructures, though the control of size and morphology relies on combined optimization of the intermolecular interactions and molecule–substrate interactions at the interface.

Since the relatively slow *drop*-cast evaporation of toluene at room temperature led to formation of 1D self-assembly of **1**, we attempted the 1D self-assembly under fast evaporation conditions. This was achieved by *spin*-casting a hot solution of **1** in toluene on the glass substrate. As shown in Fig. 1, under these conditions much thinner and elongated nanofibers were formed over the entire surface. The size and morphology are surprisingly uniform; a line-scan of one such nanofiber indicates that the diameter (*z*-height) is of only 3.1 nm (Fig. 1C and D). Based on *ab initio* calculations of the energy minimized configuration of **1** (as shown in Scheme 1), the diameter of the AEM backbone of **1** is *ca.* 2.0 nm, and the total diameter, including that of side chains, is *ca.* 4.3 nm. Considering the collapsing (folding) of the oligoethylene glycol chains, the mean diameter of **1** should be in the range of 2.0 to 4.3 nm, which is consistent with the observed size of 3.1 nm of the nanofiber. This implies that the nanofibers are composed of a single column of stacked macrocycles, the ultrafine 1D self-assembled nanostructure. Multiple, large area AFM images proved that the uniform nanofibril morphology was obtained over the entire glass surface (Fig. S2, ESI†). Formation of such a large area uniform nanopattern is likely due to enhanced wetting of toluene on the glass surface at elevated temperatures, which results in an overall lowering of surface tension.[20,21]

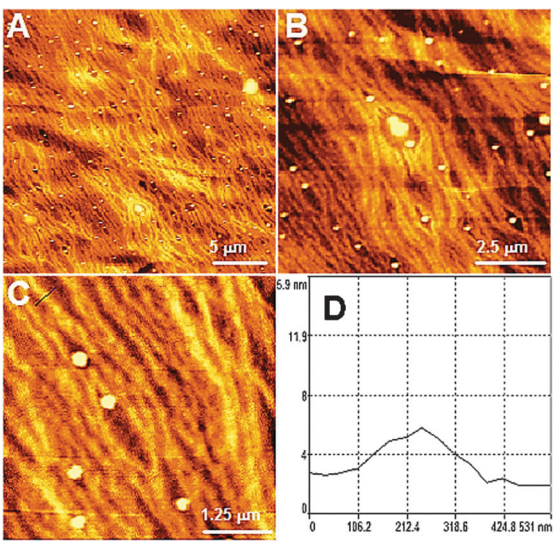

Fig. 1 Tapping mode AFM images (A–C) of the nanofibril film formed on a glass substrate by spin-casting a 1.0 mM solution of **1** in toluene (heated to 80 °C) at a speed of 1500 rpm, followed by evaporation. (D) The line scan profile as marked over one nanofiber in image C.

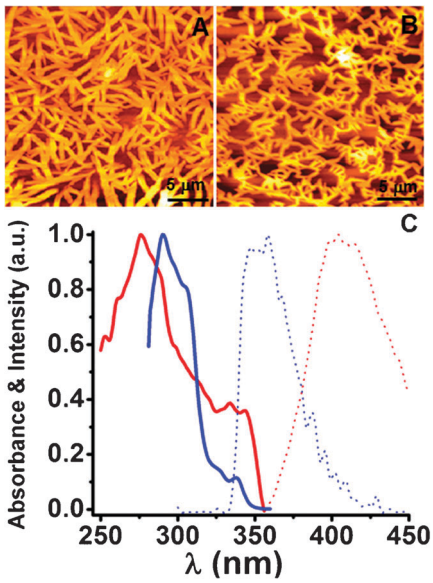

Fig. 2 Tapping mode AFM images of films formed by drop-casting a 300 μM toluene solution of **1** at room temperature (A), and 80 °C (B). Total *z*-height for images of A and B ranges from 55–70 and 32–38 nm, respectively. (C) Excitation (solid) and fluorescence (dotted) spectra of a 300 μM solution of **1** in toluene (blue), in comparison to that measured over the solid film drop-cast from a 2 mM toluene solution of **1** on quartz (red). All spectra are normalized to the maximum intensity.

To further explore the temperature effect on the self-assembly of **1**, experiments were performed by *drop*-casting toluene solutions onto the same glass surface. As shown in Fig. 2A and B, when a toluene solution of **1** was drop-cast at an elevated temperature of 80 °C, the fibril structures formed are significantly smaller (32–38 nm) compared to those formed under room temperature drop-casting (55–70 nm). The formation of smaller structures is apparently due to the fast evaporation of solvent at elevated temperature, which allows shorter time for the assembly to grow. The other factor associated with temperature, which affects the size of self-assembly, is the decrease in surface tension of toluene at elevated temperatures. This in turn results in better wetting or spreading of toluene over the glass surface.[20] A thin layer of solution of **1** apparently limits the supply of molecules for nucleation and growth of the self-assembly, thus leading to smaller diameter nanofibers, consistent with the observations of the hot *spin*-cast sample (Fig. 1).

Fig. 2C shows the fluorescence spectra of both the homogeneous solution of **1** in toluene and the crystalline aggregates (drop-cast) on a quartz slide. It is clear that the strong intermolecular π–π interactions (*i.e.* electronic coupling) result in quenching of the fluorescence of individual molecules and the formation of a new emission band at longer wavelength, associated with the aggregated states. Similar phenomena were previously observed for the assembly of other planar π-conjugated molecules, and the new emission band was assigned to an H-type aggregate.[15,22] Excitation spectra were also measured (as shown in Fig. 2C) to reveal the absorption transition property of individual molecules of **1** in comparison to the assembled state. Consistent with the fluorescence spectra, the excitation spectra exhibit a blue

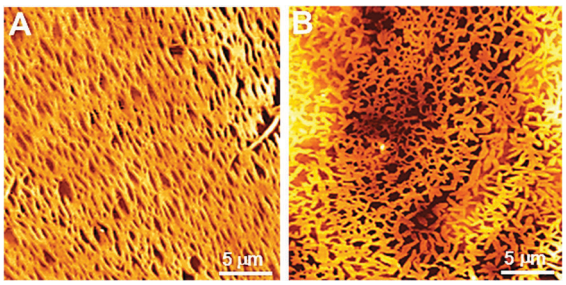

Fig. 3 Tapping mode AFM images of the films formed by drop-casting a 300 μM solution of **1** in toluene at room temperature on mica (A), and graphite (B). Total *z* height for images of A and B ranges from 35–40 and 60–65 nm, respectively.

shift of the 0–1 transition band of **1** in the solid state when compared to the solution state, implying again the H-type (cofacial) π–π stacking. Under cross-polarized light the drop-cast sample of **1** demonstrated optical anisotropy on the micron scale (Fig. S3, ESI†), similar to that observed for other planar π-conjugated molecules (*e.g.* hexabenzocoronenes).[23,24] The large scale anisotropy is consistent with the elongated fibril structure as imaged by AFM. The strong π–π stacking was further confirmed by wide angle X-ray diffraction studies as shown in Fig. S4 (ESI†), where the *d*-spacing of ~3.5 Å is characteristic of cofacial π–π stacking between planar π-conjugated molecules.[13]

In addition to the solvent effects as discussed above, the interfacial interaction between the hydrophilic PEG side-chains and the substrate also plays a critical role in affecting the self-assembly of **1** during solvent evaporation. To understand the interfacial interactions additional control experiments were performed by drop-casting a toluene solution of **1** at room temperature onto mica and graphite substrates; the former represents a typical hydrophilic surface, while the latter is extremely hydrophobic. Both of these surfaces are atomically smooth, thus ideally suited for investigating molecular assembly. It was expected that the hydrophilic side chains of **1** would interact more strongly with the mica surface compared to graphite, thus resulting in formation of distinct morphologies. Indeed, the sample cast on mica formed a fibril like nanostructure (similar to that formed on glass) upon evaporation of toluene solvent (Fig. 3A), whereas on graphite irregular nano-aggregates with varying aspect ratios were observed (Fig. 3B). Strikingly, the fibril structures formed on mica are uniform over the whole substrate as imaged using AFM. This large area uniformity is consistent with the effective wetting of toluene on mica, in conjunction with the interfacial interaction between the ethylene oxide groups and mica. In comparison, when cast on a hydrophobic graphite surface, such interfacial interaction is lacking, which prevents the fast aggregation of **1** during evaporation, *i.e.*, the surface does not play a significant role in affecting the self-assembly of **1**. Self-assembly under such conditions is similar to the process that occurs in bulk phase solutions, where irregular shapes and aggregates are formed.

In conclusion, we report on a simple, one-step fabrication of nanofibril structures on a hydrophilic surface such as glass and mica by casting a toluene solution of **1**, followed by evaporation. A systematic study using AFM revealed that the formation of shape-defined molecular assembly is a result of two concerted interactions, the solvophilic interaction between **1** and toluene, and the hydrophilic interfacial interaction between the side-chains of **1** and the polar substrate. It was found that the glass substrate at elevated temperature (*e.g.* 80 °C) provides an ideal balance between these two interactions, as well as an effective surface wetting by toluene, leading to the formation of uniform, ultrafine nanofibril structures over a large area. Structural and spectroscopic characterization indicates a long range intermolecular organization dominated by the cofacial π-stacking of the AEM cores. Such well-defined self-assembled structures shown here are a direct result of the pre-designed molecular properties of **1**. Such design and self-assembly considerations will be crucial for the advancement of AEMs in various applications.

This work was supported by DHS (2009-ST-108-LR0005) and NSF (CAREER CHE 0641353). Use of the XRD facility at the Advanced Photon Source (APS) was supported by the DOE, Office of Science, Office of Basic Energy Sciences, under Contract DE-AC02-06CH11357.

Notes and references

1 S. Hoger, *J. Polym. Sci., Part A: Polym. Chem.*, 1999, **37**, 2685.
2 Y. Che, D. E. Gross, H. Huang, D. Yang, X. Yang, E. Discekici, Z. Xue, H. Zhao, J. S. Moore and L. Zang, *J. Am. Chem. Soc.*, 2012, **134**, 4978–4982.
3 Y. Che, X. Yang, Z. Zhang, J. Zuo, J. S. Moore and L. Zang, *Chem. Commun.*, 2010, **46**, 4127–4129.
4 D. Venkataraman, S. Lee, J. Zhang and J. S. Moore, *Nature*, 1994, **371**, 591.
5 S. Hoeger, D. L. Morrison and V. Enkelmann, *J. Am. Chem. Soc.*, 2002, **124**, 6734.
6 K. Campbell, C. J. Kuehl, M. J. Ferguson, P. J. Stang and R. R. Tykwinski, *J. Am. Chem. Soc.*, 2002, **124**, 7266.
7 O. Mindyuk, M. R. Stetzer, P. A. Heiney, J. C. Nelson and J. S. Moore, *Adv. Mater.*, 1998, **10**, 1363.
8 J. Zhang and J. S. Moore, *J. Am. Chem. Soc.*, 1994, **116**, 2655.
9 S. Hoger, V. Enkelmann, K. Bonrad and C. Tschierske, *Angew. Chem., Int. Ed.*, 2000, **39**, 2268.
10 A. S. Shetty, P. R. Fischer, K. F. Stork, P. W. Bohn and J. S. Moore, *J. Am. Chem. Soc.*, 1996, **118**, 9409.
11 P. H. Ge, W. Fu, W. A. Herrmann, E. Herdtweck, C. Campana, R. D. Adams and U. H. F. Bunz, *Angew. Chem., Int. Ed.*, 2000, **39**, 3607.
12 L. Zang, Y. Che and J. S. Moore, *Acc. Chem. Res.*, 2008, **41**, 1596–1608.
13 K. Balakrishnan, A. Datar, W. Zhang, X. Yang, T. Naddo, J. Huang, J. Zuo, M. Yen, J. S. Moore and L. Zang, *J. Am. Chem. Soc.*, 2006, **128**, 6576–6577.
14 L. Zang, M. Yen, K. Balakrishnan, X. Yang and J. S. Moore, *Proc. Inst. Mech. Eng., Part N*, 2009, **223**, 139–147.
15 S. Lahiri, J. L. Thompson and J. S. Moore, *J. Am. Chem. Soc.*, 2000, **122**, 11315–11319.
16 V. Palermo, S. Morelli, C. Simpson, K. Mullen and P. Samori, *J. Mater. Chem.*, 2006, **16**, 266–271.
17 R. van Hameren, P. Schon, A. M. van Buul, J. Hoogboom, S. V. Lazarenko, J. W. Gerritsen, H. Engelkamp, P. C. M. Christianen, H. A. Heus, J. C. Maan, T. Rasing, S. Speller, A. E. Rowan, J. A. A. W. Elemans and R. J. M. Nolte, *Science*, 2006, **314**, 1433–1436.
18 R. van Hameren, J. A. A. W. Elemans, R. J. M. Nolte and A. E. Rowan, *Adv. Mater.*, 2006, **18**, 1251–1266.
19 K. Mullen and A. C. Grimsdale, *Angew. Chem., Int. Ed.*, 2005, **44**, 5592–5629.
20 D. P. Birnie, III, *J. Mater. Res.*, 2001, **16**, 1145–1154.
21 B. Charlot, S. Gauthier, A. Garraud, P. Combette and A. Giani, *J. Mater. Sci.: Mater. Electron.*, 2011, **22**, 1766–1771.
22 A. J. Fleming, J. N. Coleman, A. B. Dalton, A. Fechtenkotter, M. D. Watson, K. Mullen, H. J. Byrne and W. J. Blau, *J. Phys. Chem. B*, 2003, **107**, 37–43.
23 M. Kastler, W. Pisula, D. Wasserfallen, T. Pakula and K. Müllen, *J. Am. Chem. Soc.*, 2005, **127**, 4286–4296.
24 A. Tracz, J. K. Jeszka, M. D. Watson, W. Pisula, K. Müllen and T. Pakula, *J. Am. Chem. Soc.*, 2003, **125**, 1682–1683.

